

Damping-Driven Time Reversal for Waves

Samuel Hidalgo-Caballero^{1,2}, Surabhi Kottigegollahalli Sreenivas^{1,3}, Vincent Bacot¹, Sander Wildeman^{1,3},
Maxime Harazi¹, Xiaoping Jia¹, Arnaud Tourin¹, Mathias Fink¹, Alvaro Cassinelli⁴

Matthieu Labousse² and Emmanuel Fort^{1,*}

¹*Institut Langevin, ESPCI Paris, Université PSL, CNRS, Paris, France*

²*Gulliver, CNRS UMR 7083, ESPCI Paris, Université PSL, CNRS, 10 rue Vauquelin, 75005 Paris, France*

³*Laboratoire de Physique et Mécanique des Milieux Hétérogènes, ESPCI Paris, Université PSL, CNRS, Paris France*

⁴*School of Creative Media, City University Hong Kong, Hong Kong*



(Received 15 August 2022; accepted 24 January 2023; published 22 February 2023)

Damping is usually associated with irreversibility. Here, we present a counterintuitive concept to achieve time reversal of waves propagating in a lossless medium using a transitory dissipation pulse. Applying a sudden and strong damping in a limited time generates a time-reversed wave. In the limit of a high damping shock, this amounts to “freezing” the initial wave by maintaining the wave amplitude while canceling its time derivative. The initial wave then splits in two counterpropagating waves with half of its amplitude and time evolutions in opposite directions. We implement this damping-based time reversal using phonon waves propagating in a lattice of interacting magnets placed on an air cushion. We show with computer simulations that this concept also applies to broadband time reversal in complex disordered systems.

DOI: 10.1103/PhysRevLett.130.087201

Damping is usually associated with irreversibility in the dynamics of physical systems [1–5]. When dissipation is considered in wave propagation, wave equations are no longer time invariant under time reversal [6]. Hence, back propagation deteriorates in lossy media and challenging strategies are needed to compensate for the effect of damping [7,8]. The time-reversal counterpart of loss is gain. For instance, coherent perfect absorbers are time-reversed lasers resulting from a combination of interferences and absorption [9,10]. The interplay between gain and loss has produced unexpected fruitful features and initiated an intense research in non-Hermitian physics and parity-time (PT) symmetry [11].

In this Letter, we show that, in a lossless medium, applying a transitory dissipation for a short period of time can induce a time-reversed wave. Although energy is irreversibly lost during this process, a time reversed wave is generated when the dissipation is removed. In the following, we will call this a damping-based time reversal (DTR). This concept applies to all types of waves. It extends the family of instantaneous time mirror (ITM) techniques which was restricted to a sudden nondissipative change in the wave propagation speed (with impedance mismatch) [12]. First, we show the principle of DTR. We then provide a simple model and analyze it as a modification of the initial conditions by virtue of Cauchy’s theorem [13]. We then experimentally implement the DTR concept on phonon waves propagating in a 2D lattice of coupled magnets in the extreme case of a “freezing” dissipation pulse. Finally, we discuss these results and show by numerical simulations that DTR also applies to complex media such as highly scattering 2D elastic networks.

Figure 1 shows the principle of DTR with a broadband wave packet undergoing spreading during its propagation in a dispersive medium [Fig. 1(a)]. At time t_{DTR} , a damping shock is applied to the medium. The wave field is “frozen” and returns very slowly to a steady equilibrium state without oscillating. The damping is then removed, resulting in the creation of two counterpropagating wave packets

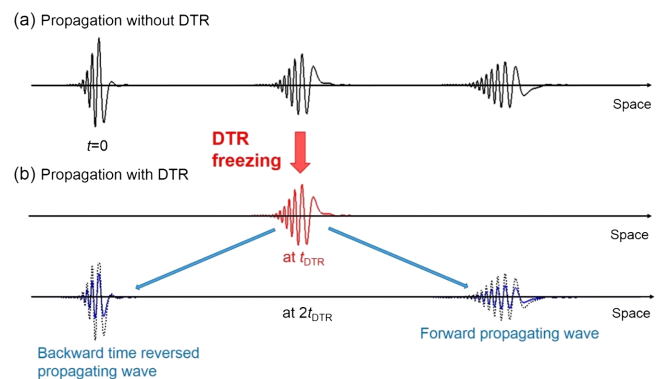


FIG. 1. Principle of a DTR mirror: (a) Propagation of a wave packet in a dispersive medium at three successive times. (b) At time t_{DTR} , a strong damping shock is applied, freezing the propagating pulse. When damping is removed, the wave packet splits into two counterpropagating pulses. At time $2t_{\text{DTR}}$, the counterpropagating wave packet (left) has the same spatial profile, with half its amplitude, as the initial one (dotted line) but propagating in the opposite direction with half its amplitude. The forward propagating wave packet (right) is identical to that of the initial pulse, with half its amplitude, propagating during $2t_{\text{DTR}}$ (dotted line) without DTR.

with half the amplitude of the initial wave field. The forward propagating packet is identical to the initial propagating pulse as if no DTR was applied, apart from the amplitude factor. The backward propagating packet is the time reversed version of the initial packet with half its amplitude. Thus, it narrows as it propagates back, reversing the dispersion effect, until the time $2t_{\text{DTR}}$, when it returns to the initial profile. It has the same spatial profile, albeit not the amplitude, as the initial wave packet but propagates in the opposite direction [see Fig. 1(b)]. The DTR process inevitably requires a loss of part of the kinetic energy of the initial wave which implies a decrease in amplitude of the time-reversed wave (and similarly of the forward propagating wave).

The DTR concept is introduced by considering waves in homogeneous nondissipative media that are usually governed by d'Alembert equation [14]. More generally, the wave field can be described by an equation in which the Laplacian operator is replaced by a more complex spatial linear operator. This type of equations can be written in the spatial Fourier space for the wave vector \mathbf{k} . Considering a time-dependent dissipation, the Fourier component of the wave field $\tilde{\phi}(\mathbf{k}, t)$ satisfies

$$\frac{\partial^2 \tilde{\phi}}{\partial t^2}(\mathbf{k}, t) + \zeta(\mathbf{k}, t) \frac{\partial \tilde{\phi}}{\partial t}(\mathbf{k}, t) + \omega_0^2(\mathbf{k}) \tilde{\phi}(\mathbf{k}, t) = 0, \quad (1)$$

with $\omega_0(\mathbf{k})$ being the angular frequency and satisfying the wave dispersion relation and $\zeta(\mathbf{k}, t)$ the time-dependent damping coefficient. To lighten the notations, the \mathbf{k} dependence is omitted in the following. In the absence of damping [$\zeta(t) = 0$], this equation has a time symmetry [$\tilde{\phi}(t)$ being a solution, $\tilde{\phi}(-t)$ also is]. This damping term can be associated with irreversibility, as it breaks the time symmetry. However, if $\zeta(t)$ remains small compared to ω_0 , an approximate reversibility is retained for times smaller than $1/\zeta(t)$ [15].

Another mathematical property may be leveraged in the large ζ limit. Let us apply a strong damping shock localized in time between t_0 and $t_1 = t_0 + \Delta t$ with a coefficient ζ_0 satisfying $\zeta_0 \gg \omega_0$, i.e., a quality factor $Q = \omega_0/\zeta_0 \ll 1$. Outside this dissipation pulse, the medium is considered lossless ($\zeta \simeq 0$). During the pulse, the last term of Eq. (1) is negligible and $(\partial \tilde{\phi}/\partial t)$ satisfies $(\partial \tilde{\phi}/\partial t)(t) = (\partial \tilde{\phi}/\partial t)(t_0) e^{-\zeta_0(t-t_0)}$. During the time interval Δt of such strong damping ($Q \ll 1$), the system behaves as an overdamped harmonic oscillator that returns very slowly to a steady equilibrium state (without oscillating), $\tilde{\phi}(t) \approx \tilde{\phi}(t_0)$. A more detailed calculation shows that in the long run limit, the wave amplitude or oscillator position decreases as $\tilde{\phi}(t) \sim \exp[-(\omega_0^2/4\zeta_0)(t-t_0)]$ [15]. To stop the “vibration” velocity but retain the oscillation position, the duration Δt of the dissipation pulse must then satisfy the freezing condition

$$\frac{1}{\zeta_0} < \Delta t < \frac{\zeta_0}{\omega_0^2}. \quad (2)$$

For high damping, Δt can thus be large compared to the period of the initial wave. The DTR process can be interpreted as a change of the initial Cauchy conditions [13]. The wave field starts evolving again with the new initial conditions at time t_1 , $(\tilde{\phi}(t_1), \partial \tilde{\phi}/\partial t(t_1)) \approx (\tilde{\phi}(t_0), 0)$ which produces two counterpropagative waves using the superposition principle [12]

$$\begin{aligned} \left(\tilde{\phi}(t_1), \frac{\partial \tilde{\phi}}{\partial t}(t_1) \right) \approx & \frac{1}{2} \left(\tilde{\phi}(t_0), \frac{\partial \tilde{\phi}}{\partial t}(t_0) \right) \\ & + \frac{1}{2} \left(\tilde{\phi}(t_0), -\frac{\partial \tilde{\phi}}{\partial t}(t_0) \right). \end{aligned} \quad (3)$$

The first term is associated (up to a factor one-half) to the exact state of the initial wave field $\tilde{\phi}_i$ before the DTR, but shifted in time $\tilde{\phi}(t > t_1) = \frac{1}{2} \tilde{\phi}_i(t + t_0 - t_1)$. The second term, with a negative sign in front of the field derivative, corresponds to the time reversed wave: $\tilde{\phi}(t > t_1) = \frac{1}{2} \tilde{\phi}_i(-t + t_0 + t_1)$. In the case of partial damping, the amplitude of both counterpropagating waves is reduced to less than half the initial one [15].

We implement a DTR with phonon waves propagating in a two-dimensional lattice. This lattice is composed of interacting magnets levitating on an air cushion on which we can apply a sudden change of damping. Figure 2 shows a schematic of the experimental setup. Each of the 200 magnetic disks is made of a small neodymium magnet (Supermagnete N35) with the same magnetic orientation and glued on top of a plastic disk of diameter 1.5 cm to obtain repulsive magnet-magnet interactions. The disks are sustained by a uniform air cushion obtained by injecting compressed air through an aluminum porous plate (Metapor BF100-AL) to drastically reduce the friction

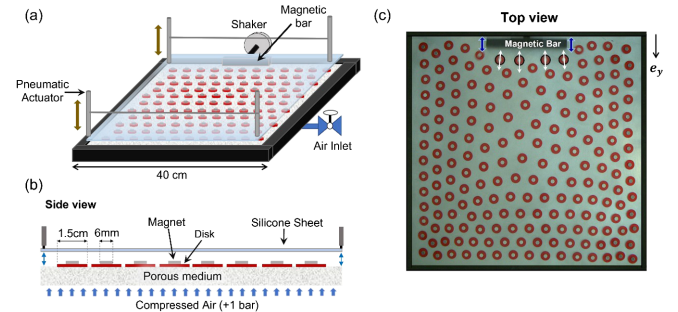


FIG. 2. (a) Schematics of the experimental setup composed of crystal of magnetically repulsive disks. (b) The friction of the disks on the table is drastically reduced by an air cushion system. The DTR on phonon waves is obtained by quickly moving down a silicone sheet to freeze the crystal. (c) Top view of the crystal excited by a magnetic bar.

coefficient with the support down to a value of $\zeta = 0.09 \pm 0.01 \text{ s}^{-1}$. This friction coefficient is measured from the relaxation time of a single disk motion in the horizontal plane $\tau = 1/\zeta \sim 10 \text{ s}$, which is much longer than that in the absence of the air cushion during the damping shock (freezing) $\tau_0 = 1/\zeta_0 < 0.002 \text{ s}$, namely, at least 1 order of magnitude smaller than the resolution limit of our camera. These disks are confined within a $L = 40 \text{ cm}$ wide square arena delimited by repulsive magnetic walls to avoid contact with the edges. At rest, the magnetic disks self-organize into a hexagonal lattice resulting from the balance between repulsion and confinement [16]. Longitudinal-like phonon waves can be excited in this lattice by moving (in the plane) a 12 cm wide magnetically repulsive bar placed on one edge [see Fig. 2(c)]. The excitation pulses are composed of 0.6 s sinusoidal arcs with an amplitude of 1.95 cm. The DTR is achieved by a vertical actuation of a translucent silicone sheet to squeeze and release the disks in a short time scale relative to their movement. The lattice motion is recorded with a camera at 50 fps (Basler acA1300-200uC) to follow the disk positions over time.

Near its equilibrium point, the lattice of magnets can be modeled with good approximation as frictionless particles that interact harmonically. The phonon waves are simulated using as initial conditions the experimental positions of the disks and of the exciting bar.

We perform a DTR experiment on a propagating phonon composed of one and two successive pulses. Figures 3(a) and 3(b) show the respective time evolutions of the longitudinal displacement averaged over the magnets surrounding the excitation source [disks with purple circles in Fig. 2(c)]. The “freezing” is performed respectively between times $t_0 = 0.60$ and $t_1 = 0.95 \text{ s}$ and time $t_0 = 1.35$ and $t_1 = 1.80 \text{ s}$, when the waves travel a distance about 20 cm to the middle of the lattice ($\sim L/2$). Note that in the evolution of the wave profile along the y axis, a forward

propagating wave is also observed with half the amplitude of the initial wave [15].

In both cases, the DTR produces a backward propagating phonon with a time-reversed profile relative to the initial phonon with approximately half the initial amplitude (see Fig. 3). No time-reversed refocusing signal is observed in the control experiment without DTR (red color). The computer simulations with harmonic interactions (dashed lines) are in good agreement with the experimental observations. From the backward phonon pulse in Fig. 3(a), we may also estimate a wave speed $c \approx (L/2)/t_0 \approx 0.33 \text{ m/s}$. For such a phonon wave with a central frequency $\sim 0.8 \text{ Hz}$, the wavelength $\lambda \approx 0.4 \text{ m}$ is much larger than lattice constant $a_0 \approx 2 \text{ cm}$. In this long wavelength limit, the characteristic harmonic pulsation $\omega_0 \approx c/a_0 \approx 16.5 \text{ s}^{-1}$ [17] which satisfies the freezing condition [Eq. (2)] $\zeta_0/\omega_0^2 > 1.8 \text{ s}$.

The experimental fidelity of the DTR can be verified by measuring the normalized cross-correlation between the initial excitation profile from 0 to t_0 and the displacement profile measured after t_1 . For both excitation profiles, we observe a maximum in the cross-correlation when the back-propagation time equals the forward-propagation time. It reaches values of 0.46 and 0.44, for the experiments with one and two excitation pulses, respectively, in close agreement with the expected value of 0.5 given by the energy conservation. The minor discrepancy is presumably due to the remaining friction between the magnets and the porous substrate as well as the imperfection of the freezing process.

DTR is expected to be independent of the complexity of the medium. To show the robustness of DTR concept, we performed computer simulations for a 2D disordered system where both longitudinal and transverse waves propagate and are strongly scattered (and coupled). This numerical model of mass spring has been introduced by Harazi *et al.* [18] to simulate the ultrasound propagation in disordered stressed granular packings. The model consists of a two-dimensional percolated lattice of point particles of mass m connected by linear springs of random stiffness. The spring constants k_s are uniformly distributed between $0.5k_s$ and $1.5k_s$, k_s being the average spring constant [Fig. 4(a)]. The masses are randomly placed on a 70×70 square network with a filling factor of 91%. Their in-plane vibrations are governed by Newton’s equation with harmonic interactions to its neighboring particles defined by their angular frequencies $\omega = \sqrt{k_s/m}$. The lattice is submitted to a static stress (tension) by pulling the four walls of the square lattice with a strain equal to 0.2 to ease the linear propagation of transverse and longitudinal elastic waves. This defines a harmonic potential for each particle of the lattice as in the experimental system. After this prestress phase, the walls are kept fixed. The network is then excited by the in-plane displacement of three particles (source) at $x = 4a$ (with a the distance between masses) with one cycle of sine at angular frequency $\omega_{exc} = 0.35\bar{\omega}$

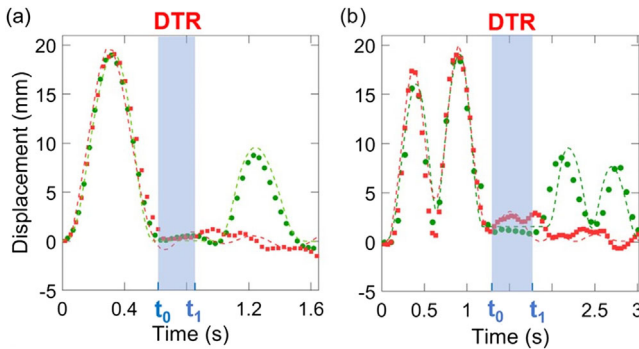


FIG. 3. DTR of a phonon wave with a single pulse profile (a) and a double pulse profile (b). Time evolution of the mean displacements in the longitudinal y direction of the four disks (with white arrows) in front of the excitation source [see Fig. 2(c)]. Experiments with DTR performed between time t_0 and time t_1 (green circles) and control experiments without DTR (red square). Associated simulations in dashed lines.

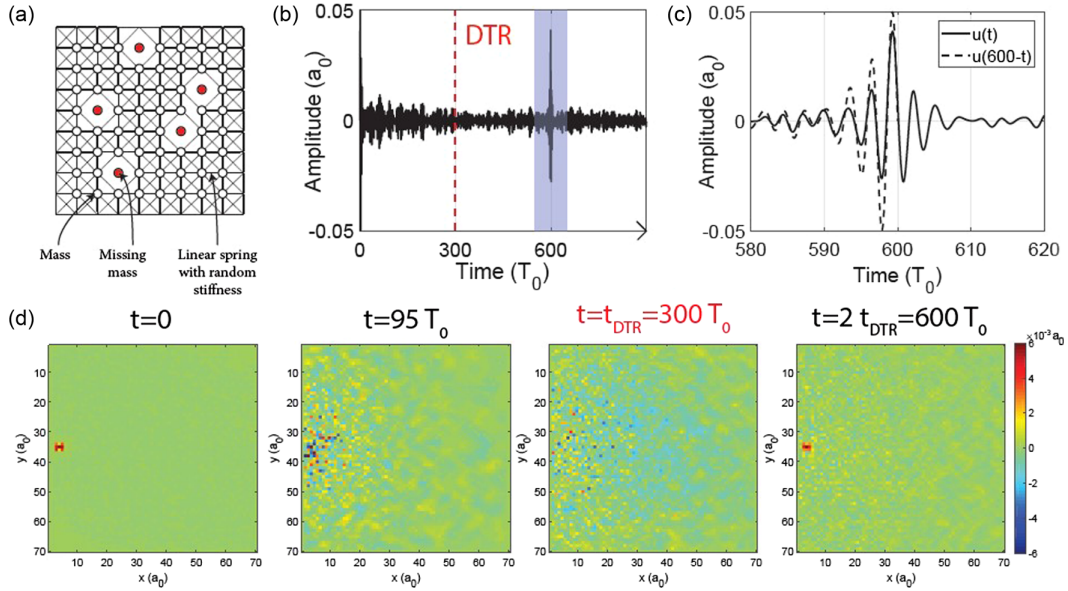


FIG. 4. (a) Schematic view of the 2D mass-spring model. (b) Time evolution of the horizontal (in-plane) displacement $u(t)$ at the source excited along x at $t = 0$ by a short pulse. DTR time: $t_{\text{DTR}} = 300 T_0$ (red dashed line). (c) Close-up of (b) around the refocusing time $600 T_0$. The black dashed line represents $u(600 - t)$. (d) Panels representing the field displacement of the source at $t = 0$ (initial time), $95T_0$, $t_{\text{DTR}} = 300 T_0$ (during the freezing shock) and $t = 600 T_0$ (refocusing time). Lengths are expressed in units of lattice constant a_0 .

with $\bar{\omega} = \sqrt{k_s/m}$. Figures 4(b) and 4(d) show the time evolution of the in-plane displacement of the source and of the associated wave field at various times, respectively. At $t = 0$, the motion is confined to the source. Then, the source motion decreases rapidly at a noise level of approximately one-tenth of its initial value. The initial perturbation propagates either at longitudinal wave or transverse wave speeds [19] and is strongly scattered in the inhomogeneous mass-spring network at long-time propagation. At time $t = 95 T_0$, the perturbation spreads through the network and the particle motions become randomly distributed. The network acts as a complex disordered medium due to the random spring stiffnesses and the random vacancies in the squared network. When the DTR is applied at $t_{\text{DTR}} = 300 T_0$, all the particle velocities are set to zero, as if an infinite damping was applied instantaneously, keeping only the potential energy in the system. Immediately after, the masses are released with zero velocity [third panel Fig. 4(d)]. The particles undergo complex motions until a coherent field appears refocusing on the initial source around time $t = 2t_{\text{DTR}} = 600 T_0$ [fourth panel in Fig. 4(d)]. The horizontal displacement of the source undergoes a very sharp increase reaching approximately 80% of its initial value [Fig. 4(c)]. The converging wave then diverges again, creating a new complex displacement field. The refocusing is also observed in time at $t = 2t_{\text{DTR}}$ [see Fig. 4(c)].

The DTR process results from the decoupling of the initial wave field from its time derivative. The kinetic energy associated with the time derivative of the field

$\partial\tilde{\phi}_i/\partial t$ vanishes when the dissipation is activated while the potential energy associated to the wave field $\tilde{\phi}_i$ remains unchanged. In the case of an initially propagating wave, the energy of the wave is equally partitioned between potential and kinetic energy. Thus, half of the initial energy is lost in the DTR process resulting in a quarter of the initial energy being TR while another quarter forward propagating. However, the refocusing signal can still reach 80% of the initial amplitude as measured in the simulations [see Fig 4(c)]. This apparent contradiction results from the interferences between the refocusing wave and the rediverging one which produce a standing wave field alternating kinetic and potential energy [15]. Note that during propagation in a complex medium, scattering induces interferences which similarly induce fluctuations in the energy partition of the wave field.

The Cauchy analysis in terms of initial conditions to determine the wave field evolution enables one to make a link with Loschmidt's gedanken experiment for particles evolution [20]. Loschmidt imagined a demon capable of instantaneously reversing the velocity of the particles of a gas while keeping their position unaffected and, thus, time reversing the gas evolution [20,21]. Although this scheme is impossible in the case of particles due to the extreme sensitivity to initial conditions, it is more amenable for waves because they can often be described with a linear operator and any error in initial conditions will not suffer from chaotic behavior. The wave analogue of this Loschmidt demon changes Cauchy's initial conditions $(\phi_i, \partial\phi_i/\partial t)$ to $(\phi_i, -\partial\phi_i/\partial t)$. Upon freezing, the wave

field initial conditions are reset with a null time derivative but because of the superposition principle [see Eq. (3)], the DTR produces a time-reversed wave as a Loschmidt demon. The DTR concept is generic and applies even in the case of complex inhomogeneous materials as shown in the 2D simulations (see Fig. 4) since the superposition principle is independent of the complexity of the medium.

In contrast with the ITM approach based on wave velocity changes [12] and standard digital time reversal methods [22], the backward propagating wave is directly proportional to the TR of the original wave and not to the time reversal of its time derivative or antiderivative. From that perspective, DTR has thus no spectral limitations and can be applied to broadband wave packets. This results in a higher fidelity and enhanced broadband capabilities compared to other methods [12,22].

The limitation in time-reversing wide spectral range comes from the ability to freeze the field sufficiently rapidly in comparison with the phase change in the wave packet, resulting in the maximum value for the angular frequency $\omega_0 \ll \zeta$. The DTR principle could be applied to any type of waves such as in optics by changing abruptly the conductivity of the medium [23], or in acoustics by using varying electrorheological medium [24].

We are very grateful to Y. Couder and A. Eddi for fruitful and stimulating discussions. We thank A. Fourgeaud for his help in building the experimental setup. S. K. S. thanks the French Embassy in India for Charpak scholarship. S. H. C., M. L., and E. F. thank the EU MSCA H2020 COFUND UpToParis No. 754387 program and CONACYT Mexico. The authors acknowledge the support of the AXA Research Fund. This work has received support under the program “Investissements d’Avenir” launched by the French Government.

*Corresponding author.
emmanuel.fort@espci.fr

- [1] R. Landauer, Irreversibility and heat generation in the computing process, *IBM J. Res. Dev.* **5**, 183 (1961).
- [2] M. Fink, G. Montaldo, and M. Tanter, Ultrasonic time reversal mirrors, *AIP Conf. Proc.* **728**, 514 (2004).
- [3] R. Kubo, The fluctuation-dissipation theorem, *Rep. Prog. Phys.* **29**, 255 (1966).
- [4] E. Celeghini, M. Rasetti, and G. Vitiello, Quantum dissipation, *Ann. Phys. (N.Y.)* **215**, 156 (1992).
- [5] H. B. Callen and T. A. Welton, Irreversibility and generalized noise, *Phys. Rev.* **83**, 34 (1951).
- [6] M. Fink, Time-reversal acoustics in complex environments, *Geophysics* **71**, SI151 (2006).
- [7] H. Ammari, E. Bretin, J. Garnier, and A. Wahab, Time reversal in attenuating acoustic media, *Contemp. Math.* **548**, 151 (2011).
- [8] Y. Labyed and L. Huang, Ultrasound time-reversal MUSIC imaging with diffraction and attenuation compensation, *IEEE Trans. Ultrason. Ferroelectr. Freq. Control* **59**, 2186 (2012).
- [9] W. Wan, Y. Chong, L. Ge, H. Noh, A. D. Stone, and H. Cao, Time-reversed lasing and interferometric control of absorption, *Science* **331**, 889 (2011).
- [10] Y. D. Chong, L. Ge, H. Cao, and A. D. Stone, Coherent Perfect Absorbers: Time-Reversed Lasers, *Phys. Rev. Lett.* **105** (2010).
- [11] R. El-Ganainy, K. G. Makris, M. Khajavikhan, Z. H. Musslimani, S. Rotter, and D. N. Christodoulides, Non-Hermitian physics and PT symmetry, *Nat. Phys.* **14**, 11 (2018).
- [12] V. Bacot, M. Labousse, A. Eddi, M. Fink, and E. Fort, Time reversal and holography with spacetime transformations, *Nat. Phys.* **12**, 972 (2016).
- [13] J. Hadamard, *Lectures on Cauchy’s Problem in Linear Partial Differential Equations* (Dover Publications, New York, 2003).
- [14] F. S. Crawford, *Berkeley Physics Course. Vol. 3, Waves* (McGraw-Hill, New York, 1968).
- [15] See Supplemental Material at <http://link.aps.org/supplemental/10.1103/PhysRevLett.130.087201> for supplemental figures and model.
- [16] M. Berhanu, S. Merminod, G. Castillo, and E. Falcon, Wave spectroscopy in a driven granular material, *Proc. R. Soc. A* **478**, 20220014 (2022).
- [17] C. Kittel, *Introduction to Solid State Physics Eighth Edition* (Wiley, London, 2021).
- [18] M. Harazi, *Multiple Scattering and Time Reversal of Ultrasound in Dry and Immersed Granular Media*, (University Paris Diderot, 2017).
- [19] M. Harazi, Y. Yang, M. Fink, A. Tourin, and X. Jia, Time reversal of ultrasound in granular media, *Eur. Phys. J. Spec. Top.* **226**, 7 (2017).
- [20] J. Loschmidt, Über Den Zustand Des Warmegleichgewichtes Eines Systems von Körpern Mit Rücksicht Auf Die Schwerkraft, *Sitz. Math.-Naturwiss. Cl. Akad. Wiss., Wien* **73**, 128 (1876).
- [21] P. L. Marston, Maxwell–Thomson–Loschmidt reversal, *Nat. Phys.* **13**, 2 (2017).
- [22] M. Fink, Time-reversal waves and super resolution, *J. Phys. Conf. Ser.* **124**, 012004 (2008).
- [23] J. Wilson, F. Santosa, M. Min, and T. Low, Temporal control of graphene plasmons, *Phys. Rev. B* **98**, 081411(R) (2018).
- [24] L. Li, M. Wang, J. Wang, and X. Zhao, The control of ultrasonic transmission by the metamaterials structure of electrorheological fluid and metal foam, *Smart Mater. Struct.* **26**, 115006 (2017).